Available online at www.sciencedirect.com

ScienceDirect

Procedia CIRP 124 (2024) 513–517

www.elsevier.com/locate/procedia

13th CIRP Conference on Photonic Technologies [LANE 2024], 15-19 September 2024, Fürth, Germany

Investigating the effect of laser power modulation in transient states during fusion cutting of 10 mm thick AISI304

Matteo Busatto[a]*, Sofia Guerra[a], Leonardo Caprio[a], Barbara Previtali[a]

[a]*Department of Mechanical Engineering, Politecnico di Milano, Via La Masa 1, 20156 Milan, Italy*

* Corresponding author. *E-mail address:* matteo.busatto@polimi.it

Abstract

In fusion laser cutting of intricate geometries, the processing speed often varies significantly from its nominal value due to inherent machine dynamics. These variations can lead to excessive energetic input and drifts from the reference cut quality. To address defect formation during transient conditions, a conventional approach involves power reduction to compensate for speed variations. This help prevent thermal imbalances and material overheating issues, ultimately preserving the final cut's quality. An alternative solution is based on pulsed wave emission, providing dynamic and precise control over the thermal energy delivered to the workpiece. In this work, pulsed wave emission was employed to ensure process stability during transient conditions for fusion cutting of 10mm AISI304. A 6kW fiber laser was utilized alongside a coaxial camera-based monitoring setup to observe the melt dynamics. Results demonstrate that power modulation effectively reduces defect formation, and process emission images can be exploited to identify successful cuts.

Keywords: Fusion laser cutting, pulsed wave emission, stainless steel

1. Introduction

Nowadays, laser fusion cutting stands as one of the most widespread manufacturing processes in the metal working industry. In fusion laser cutting of intricate geometries, processing speed exhibits significant variations with respect to the nominal value due to the inherent machine dynamics, causing excessive energetic input and drifts from the reference cut quality. Today, the degradation of cut quality in transient state conditions stands as one of the most significant issues since real-time modification of the process parameters is required to avoid defect formation. Amongst the viable solutions to regulate the energy delivered to the material the use of temporal modulation of the laser emission power offers quick response times and a scalable response to regulate the thermal input. Temporal modification of the emission profile is exploited to tailor the process outcome throughout various laser-based processes (including welding, micromachining and powder bed fusion) [1,2]. With regards to laser cutting, however, the majority of the literature studies explored the effects of continuous wave (CW) emission on part quality, while only a few works investigated the impact of temporal modulation [3,4,5,6]. To date, no publications have addressed pulsed wave emission as a possible solution to reduce quality defects in transient state conditions.

Moreover, considering the interest in developing intelligent and fully automated laser cutting systems, the use of monitoring tools to extract process relevant information has an elevated appeal from an industrial perspective. In literature there is evidence that such information may be exploited to develop closed-loop control of laser cutting process, as introduced by *Pacher et al.* [7,8,9] and *Levichev et al.* [10,11,12]. The coaxial-based camera monitoring enables the real-time assessment of cut quality by analysing geometrical features extracted from process emission images that were obtained at different levels of cutting speed. However, the combined impact of the cutting velocity and temporal emission modulation has not been

10.1016/j.procir.2024.08.164

explored alongside with the possible effects over the melt dynamics and plasma formation phenomena.

The scope of this work is to explore the feasibility of using pulsed wave emission to minimise defect formation at different levels of cut velocity (representative of transient conditions) during the fusion cutting of 10 mm thick AISI304 stainless steel. Moreover, a coaxial camera-based monitoring setup has been used to observe the melt dynamics, aiming to establishing a correlation between part quality and geometrical features extracted from process emission images.

2. Materials and Methods

2.1. Materials

The material employed was 10 mm thick stainless steel AISI304. The nominal composition is reported in Table 1.

Table 1. Chemical composition of stainless steel AISI304 (wt%).

C	Mn	Si	P	S	Cr	Ni	N	Fe
0.07	2.00	1.00	0.05	0.02	19.0	10.5	0.11	balanced

2.2. Laser cutting and monitoring system

The experiments were performed on a customized version of the LC5 laser cutting machine (*Adige-SYS, BLMGroup, Levico Terme, Italy*). An industrial high-power multi-mode fiber laser source capable of delivering up to 6 kW of power at 1070 nm (*YLS-6000-CUT, IPG Photonics Coorp., Oxford, Massachusetts*) was employed. The transport fiber (d_{core} = 100 µm) was coupled to an HPSSL cutting head (*Precitec GmbH & Co., Gaggenau, Germany*). The specifications of the laser system are reported in Table 2.

Table 2. Laser cutting and monitoring system specifications.

Laser system specifications	Values
Maximum emission power, P_{max} [W]	6000
Beam quality factor, M^2	11.7
Collimation lens, f_{col} [mm]	100
Focal lens, f_{foc} [mm]	200
Fiber core diameter, d_{core} [µm]	100
Beam waist diameter, d_{waist} [µm]	200
Monitoring system specifications	**Values**
Field of view, [px x px]	320 x 320
Spatial resolution, [µm/px]	9.6
Acquisition frequency, [Hz]	750

An industrial camera was coaxially integrated in the cutting head for monitoring purposes, as represented in Fig. 1a. The selected camera sensor is an industrial CMOS camera (*xiQ MQ013MG-ON, Ximea GmbH, Münster, Germany*) based on Si photodetectors. Monochrome images with 8 bit depth were acquired at 750 fps. Moreover, a near infrared wavelength range was selected by incorporating band pass and short pass filters centred at 750 nm and 1000 nm, respectively. Monitoring system parameters are reported in Table 2. A series of geometrical features was derived through the analysis of video frames capturing process emissions. These features are extracted from binary images after hard thresholding of the grayscale images at predetermined values. The threshold value employed by *Pacher et al.* [8], set to 15, which represents the pixel intensity of the grayscale matrix after analog-to-digital conversion, was maintained in this work. Examples of extracted features include blob width and centroid coordinates, as depicted in Fig. 1b. For each process condition, geometric features are extracted from all captured frames.

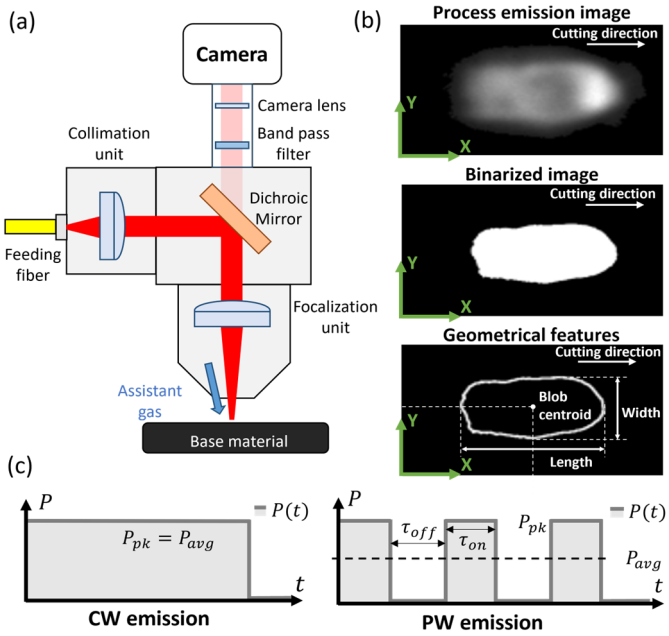

Figure 1. (a) Monitoring architecture scheme; (b) Graphical representation of the geometrical features extracted from process emission images; (c) Temporal profile for CW and PW emission modes for 50% duty cycle ($\tau_{on} = \tau_{off}$).

A schematic representation of the laser temporal profile for CW and PW square-wave emission is reported in Fig. 1c. The duty cycle can be defined as the fraction of time during which laser pulse emission occurs:

$$\delta = \tau_{on}/(\tau_{on} + \tau_{off}) \quad (1)$$

where τ_{on} is the pulse duration and τ_{off} is the laser off time between two consecutive pulses. Moreover, the duty cycle can be explicitly related to the modulation frequency as:

$$\delta = \tau_{on} \cdot f \quad (2)$$

The modulation frequency is defined as:

$$f = 1/(\tau_{on} + \tau_{off}) \quad (3)$$

Finally, the average power output delivered by the laser source during pulsed wave emission is strictly related to the duty cycle value and can be defined as:

$$P_{avg} = P_{pk} \cdot \delta \quad (4)$$

2.3. Experimental plan

In this work, the effect of modifying the laser emission power by varying the duty cycle was investigated during the cutting of 10 mm AISI304. First, a reference process condition was experimentally identified to maximize processing speed and minimize dross formation during CW emission (δ = 100%). The 6 kW laser beam was focused at 11 mm below the nozzle, with a stand-off distance of 0.7 mm from the metal sheet. A gas

pressure of 17 bar was used. The fixed process parameters are reported in Table 3.

Moreover, to simulate transient velocity conditions, cuts at different levels of speed were conducted. With respect to the reference condition at 1.3 m/min cutting velocity and 100% duty cycle, four other decreasing levels of speed were considered. In order to evaluate the effect of power modulation, a factorial design considering five levels of duty cycle was designed, as reported in Table 3. Based on a preliminary investigation, a fixed modulation frequency of 500 Hz was selected, resulting in a pulse duration (τ_{on}) ranging from 0.8 ms (δ = 40%) to 1.7 ms (δ = 85%).

Each processing condition was replicated three times resulting in a total of 75 samples. The samples obtained under different operating conditions were visually inspected and three categorical conditions were identified:

- Loss of cut: the molten material is not ejected from the kerf but resolidified, preventing material separation.
- Successful cut: the molten material is ejected, leading to complete material separation.
- Plasma cut: unstable laser cutting process conditions may induce plasma formation, resulting in complete material separation but with low cut-edge quality [13].

Representative optical microscope image of these conditions are reported in Fig. 3 (loss of cut shown in a top view, while plasma and successful cut showing the kerf surface).

The process emission images obtained from the coaxial monitoring setup, alongside with their geometrical features, were then analyzed to detect correlations useful to discern the different processing conditions. In particular, the features selected for this study are blob width and centroid coordinates (X and Y) along with overall grayscale blob intensity. Additionally, for successful conditions, the samples were characterized in terms of roughness and dross (see Fig. 2).

Table 3. Experimental campaign.

Fixed parameters	
Laser power, P [W]	6000
Frequency, f [Hz]	500
Assistant gas	N_2
Gas pressure, Pr [bar]	17
Focal position, FP [mm]	-11
Stand-off Distance, SOD [mm]	0.7
Variable parameters	
Cutting speed, v [m/min]	0.9; 1.0; 1.1; 1.2; 1.3
Duty cycle, δ [%]	40; 55; 70; 85; 100

2.4. Characterization and measurement

The surface roughness was measured with a Mahr PGK perthometer profilometer equipped with an MFW-250 feeler and a 2 µm radius tip. In accordance with UNI EN ISO9013:2017 standard, the acquired sample primary profile was filtered at 0.8 mm cut-off wavelength. The resulting mean peak to valley height roughness profile R_z, was measured at 1/3 of the material thickness from the top edge, as represented in Fig. 2a. The Echo-Lab Optical Microscope (*Echo-Lab SM 535 H, Devco S.r.l., Milan, Italy*) was employed for high-resolution imaging of cut edge profiles, while the dross defect was estimated through the MATLAB analysis of the cut edge images taken with the Mitutoyo microscope (*Mitutoyo Quick Vision PRO ELF QV-202*). An example is provided in Fig. 2b.

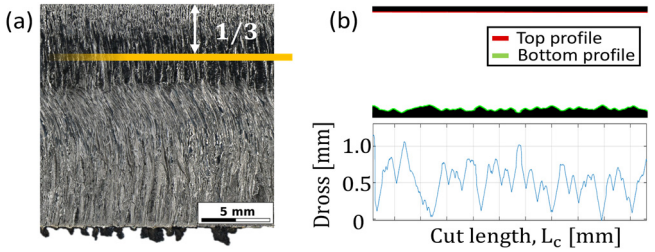

Figure 2. (a) Surface roughness measurement; (b) Dross defect estimation.

3. Results

3.1. Part quality evaluation

The samples obtained under different operating conditions were visually inspected and three categorical conditions were identified. The categorical results are reported in the feasibility map presented in Fig. 3 as a function of the duty cycle and cutting speed.

As the duty cycle decreases, the power delivered to the workpiece material diminishes (in accordance with equation 4). This reduces the specific energy delivered to the material which is related to the P_{avg}/v ratio as defined in the lumped heat capacity model by *Steen and Mazumder* [14]. From the feasibility region shown in Fig. 3, it is clear that an increase in cutting velocity or a reduction of the duty cycle cause unstable plasma cut conditions and eventually lead to loss of cut, indicating the significance of this ratio in determining a successful process outcome. Consequently, as the average power decreases, it becomes necessary to reduce the speed to maintain a successful cutting condition.

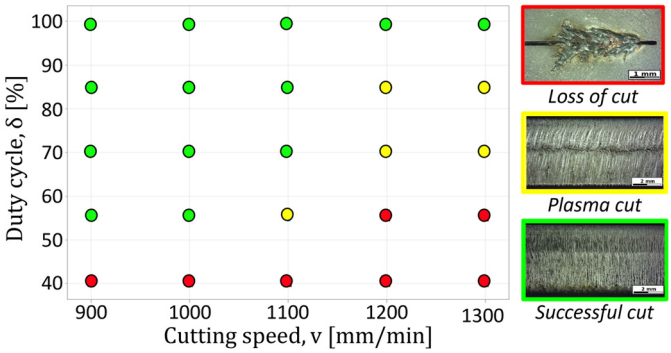

Figure 3. Process feasibility map: Successful cut (in green), Plasma cut (in yellow) and Loss of cut (in red).

On the other hand, reducing the cutting speed whilst maintaining a constant level of power (situation which typically occurs in real case scenarios due to the inherent machine dynamics when changing direction or processing complex geometries) does not impinge on the process feasibility. The effect of such condition was assessed in terms of dross formation and profile roughness which are shown in Fig. 4 as a function of the process parameters for the successful cut conditions. The profile roughness (Fig. 4a) is not significantly affected by the duty cycle and cutting speed. However, dross formation notably increases when the cutting speed is reduced whilst maintaining CW emission (as visible in

Fig. 4b). When the cutting speed is reduced, dross formation may be mitigated by employing a lower level of duty cycle. At 1.3 m/min and 1.2 m/min, the only successful cut condition corresponds to the one employing CW emission indicating a non-sufficient P_{avg}/v ratio. At 1.1 m/min, δ=100% still results in the most favorable condition from the dross formation perspective, whilst at lower levels of speed the use of a reduced level of duty cycle (δ=85%) diminishes the defect. Thus it emerges that a minimum level of the specific energy delivered to the material (regulated by the P_{avg}/v ratio) is capable of defining the lower level of the process feasibility region.

On the other hand, elevated levels of the P_{avg}/v ratio are responsible for higher dross formation. Hence, by modulating the emission power it is possible to mitigate defect formation at different levels of cut velocity and this may be implemented as an effective strategy to avoid dross generation during transient conditions caused by directional changes or the cutting of complex and intricate geometries. Moreover, the use of temporally modulated emission impacts on the melt dynamics. Rapid variations of the power (such in the case of square waveform employed in the present work) cause a modification of the surface temperature. As shown by *Caprio et al.* [16], this affects the recoil pressure exerted over the liquid metal and may aid in the expulsion mechanism of the melt thus mitigating dross formation. This may thus explain the reduced defect formation. However, if the energetic input is not sufficient, this will imply an overall loss of penetration thus leading to localized plasma formation.

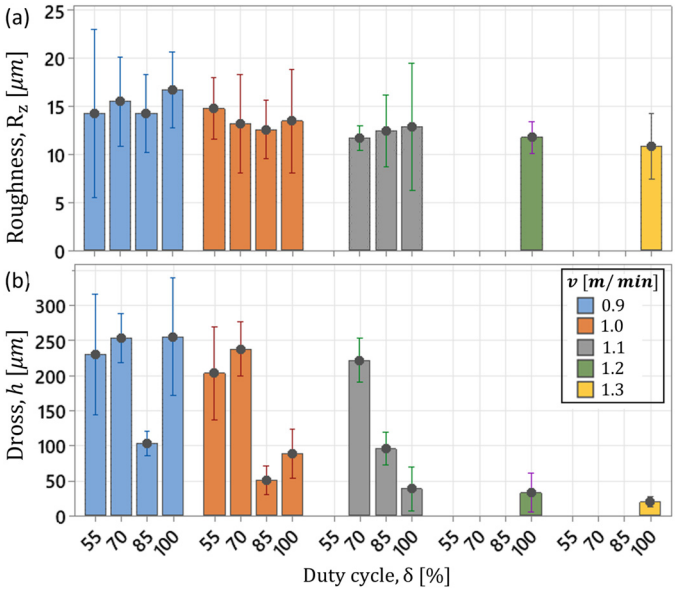

Figure 4. Part quality evaluation: (a) Roughness defect, (b) Dross defect.

3.2. Melt pool geometrical analysis

Representative video frames showing the process emission in the different operating conditions are reported in Fig. 5. The loss of cut condition may be clearly distinguished from the other processing conditions. In the region of the image where the laser-material interaction is occurring, frames from the plasma cut condition show higher intensities with respect to successful cuts. Such information may be exploited for the detection of loss of cut conditions previously done by *Levichev et al.* exploiting a photodiode sensing system [10]. It is thus evident that sensing of the process emission provides valuable information regarding the state of the cut and that it may be possible to exploit the geometrical features to perform such classification.

When the cutting speed is reduced with respect to the reference condition, the higher value of the specific energy leads to a straighter cutting front and a corresponding easier melt removal. As a matter of fact, at a fixed level of duty cycle a decrease in the melt pool intensity can be observed in Fig 5 as the velocity is lowered. Conversely, faster processing conditions change the cutting front inclination, resulting in an increased proportion of the melt pool observable via the coaxial monitoring set up. This occurs due to the lower inclination of the kerf, which may be correlated to an insufficient level of the P_{avg}/v ratio. Moreover, an excessive reduction of the duty cycle leads to insufficient specific energy to achieve the keyhole penetration required to obtain stable cutting conditions. This phenomenon generates an increase in the absorption of the laser beam by the melt layer, thus causing plasma formation which is highly detrimental on part quality [13].

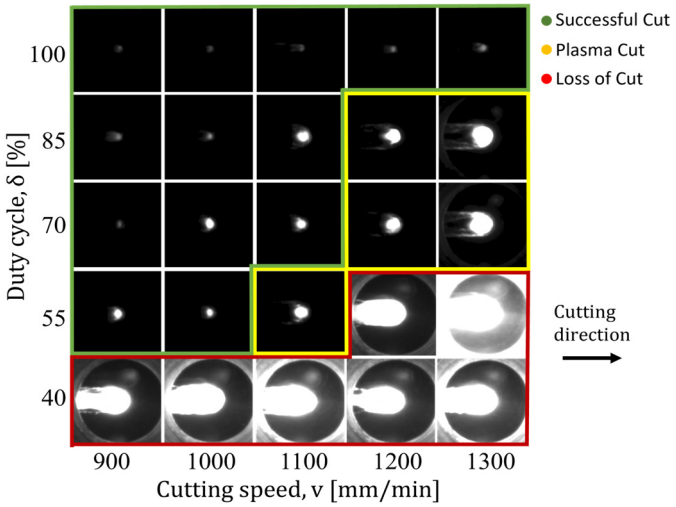

Figure 5. Process emission images under different working conditions. Successful cut (in green), Plasma cut (in yellow) and Loss of cut (in red).

Plasma formation alongside with the changing inclination of the front kerf geometry significantly increases the intensity of the process emission captured by the monitoring system. As a matter of fact, plasma cut conditions can be distinguished as they present a greater width of the process emission blob and brighter images compared to the successful cut conditions. Loss of cut on the other hand, show an even more significant amount of radiation emitted towards the sensor allowing to discern also the nozzle geometry. The significant increase in terms of the melt pool size and geometry and as well as the process emission radiation may be employed to categorize the cutting state by combining the information provided. The selected features are shown graphically in the scatterplot matrix of Fig.6. Observing the clustering of the data points that allow to discern between the different process conditions, it is possible to envision the use of classification algorithms to perform an automated detection of the process state based on the geometrical and intensity features of the images. Supervised machine learning approaches may thus be employed to train algorithms capable of detecting in real-time critical defect formation and guarantee successful outcome of the process.

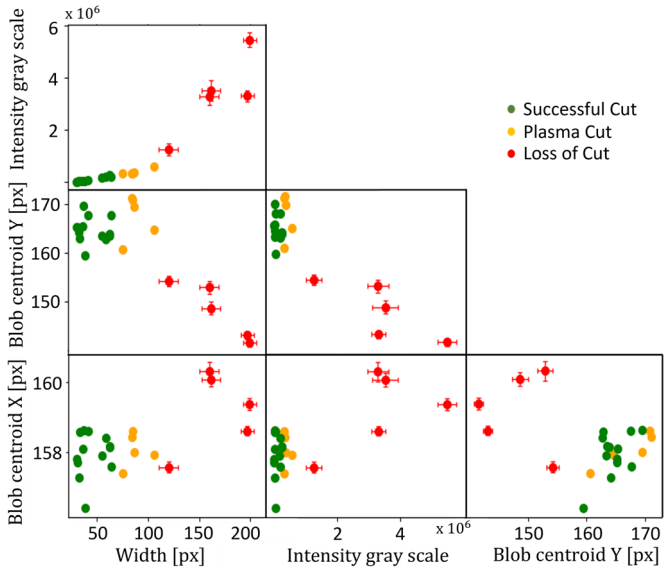

Figure 6. Scatterplot of the different cutting conditions for the extracted features: Successful cut (in green), Plasma cut (in yellow) and Loss of cut (in red). For each feature, the mean value and standard error interval are considered.

4. Conclusions

The present work explores the impact of laser power modulation during the fusion cutting of 10 mm thick AISI304 stainless steel. When the cutting speed is reduced, the use of temporal modulation can prevent excessive dross formation by reducing the specific energetic input to the workpiece. This approach could provide an effective solution for addressing quality degradation which are generated by variations in the cut speed imposed by changes of geometry or direction. Moreover, coaxial camera monitoring allowed to capture the variations in terms of process emission. The geometrical features and intensity of the acquired frames may be exploited in future to determine in real-time the actual state of the process, guaranteeing a successful cut and allowing the machine to regulate process parameters to avoid plasma or loss of cut conditions. Hence, future works will leverage such information to train machine learning algorithms for the automatic and real-time classification of the process conditions.

Acknowledgements

The authors gratefully acknowledge the BLM Group for supporting the research activities. Additionally, the authors would like to acknowledge the Italian Ministry for University and Research (MUR) for supporting the research through the National Plan for Recovery and Resilience (PNRR).

References

[1] L. Caprio, A. G. Demir, and B. Previtali, ‘Influence of pulsed and continuous wave emission on melting efficiency in selective laser melting’, *Journal of Materials Processing Technology*, vol. 266, pp. 429–441, Apr. 2019, doi: 10.1016/j.jmatprotec.2018.11.019.

[2] E. Assuncao and S. Williams, ‘Comparison of continuous wave and pulsed wave laser welding effects’, *Optics and Lasers in Engineering*, vol. 51, no. 6, pp. 674–680, Jun. 2013, doi: 10.1016/j.optlaseng.2013.01.007.

[3] K. A. Ghany and M. Newishy, ‘Cutting of 1.2mm thick austenitic stainless steel sheet using pulsed and CW Nd:YAG laser’, *Journal of Materials Processing Technology*, vol. 168, no. 3, pp. 438–447, Oct. 2005, doi: 10.1016/j.jmatprotec.2005.02.251.

[4] A. F. M. Tahir and S. N. Aqida, ‘An investigation of laser cutting quality of 22MnB5 ultra high strength steel using response surface methodology’, *Optics & Laser Technology*, vol. 92, pp. 142–149, Jul. 2017, doi: 10.1016/j.optlastec.2017.01.005.

[5] Lv. Shanjin and W. Yang, ‘An investigation of pulsed laser cutting of titanium alloy sheet’, *Optics and Lasers in Engineering*, vol. 44, no. 10, pp. 1067–1077, Oct. 2006, doi: 10.1016/j.optlaseng.2005.09.003.

[6] A. H. A. Lutey, A. Ascari, A. Fortunato, and L. Romoli, ‘Long-pulse quasi-CW laser cutting of metals’, *Int J Adv Manuf Technol*, vol. 94, no. 1–4, pp. 155–162, Jan. 2018, doi: 10.1007/s00170-017-0913-x.

[7] M. Pacher, S. Strada, M. Tanelli, B. Previtali, and S. M. Savaresi, ‘Real-time velocity regulation for productivity optimization in laser cutting’, *IFAC-PapersOnLine*, vol. 54, no. 1, pp. 1230–1235, 2021, doi: 10.1016/j.ifacol.2021.08.146.

[8] M. Pacher, L. Franceschetti, S. C. Strada, M. Tanelli, S. M. Savaresi, and B. Previtali, ‘Real-time continuous estimation of dross attachment in the laser cutting process based on process emission images’, *Journal of Laser Applications*, vol. 32, no. 4, p. 042016, Nov. 2020, doi: 10.2351/7.0000145.

[9] M. Pacher *et al.*, ‘Real-time roughness estimation in laser oxidation cutting via coaxial process vision’, 2023.

[10] N. Levichev, G. C. Rodrigues, and J. R. Duflou, ‘Real-time monitoring of fiber laser cutting of thick plates by means of photodiodes’, *Procedia CIRP*, vol. 94, pp. 499–504, 2020, doi: 10.1016/j.procir.2020.09.171.

[11] N. Levichev, G. Costa Rodrigues, V. Vorkov, and J. R. Duflou, ‘Coaxial camera-based monitoring of fiber laser cutting of thick plates’, *Optics & Laser Technology*, vol. 136, p. 106743, Apr. 2021, doi: 10.1016/j.optlastec.2020.106743.

[12] N. Levichev, A. Tomás García, and J. R. Duflou, ‘Monitoring Opportunities in Fiber Laser Flame Cutting’, *Lasers Manuf. Mater. Process.*, vol. 8, no. 4, pp. 491–510, Dec. 2021, doi: 10.1007/s40516-021-00158-y.

[13] E. Fallahi Sichani, S. Kohl, and J. R. Duflou, ‘Plasma detection and control requirements for CO 2 laser cutting’, *CIRP Annals*, vol. 62, no. 1, pp. 215–218, 2013, doi: 10.1016/j.cirp.2013.03.029.

[14] W. M. Steen and J. Mazumder, *Laser Material Processing*. London: Springer London, 2010. doi: 10.1007/978-1-84996-062-5.

[15] N. Levichev, G. Costa Rodrigues, R. Dewil, and J. R. Duflou, ‘Anticipating heat accumulation in laser oxygen cutting of thick metal plates’, *Journal of Laser Applications*, vol. 32, no. 2, p. 022018, May 2020, doi: 10.2351/7.0000052.

[16] L. Caprio, A. G. Demir, and B. Previtali, ‘Understanding the effects of temporal waveform modulation of the laser emission power in laser powder bed fusion: Part I - Analytical modelling’, *J. Phys. D: Appl. Phys.*, vol. 55, no. 49, p. 495101, Dec. 2022, doi: 10.1088/1361-6463/ac984c.